JOURNAL OF MATERIALS SCIENCE **40** (2005) 6391–6397

Determination of the alloy scattering potential in modulation-doped $In_{0.53}Ga_{0.47}As/In_{0.52}Al_{0.48}As$ heterojunctions from magnetotransport measurements

E. TIRAŞ*†, S. ALTINÖZ, M. CANKURTARAN, H. ÇELİK
Department of Physics, Hacettepe University, Beytepe, 06800 Ankara, Turkey
E-mail: engin@hacettepe.edu.tr

N. BALKAN
Semiconductor Optoelectronics Group, Department of Electronic Systems Engineering, University of Essex, 3SQ CO4 Colchester, UK

Published online: 25 October 2005

The results of magnetotransport measurements are used to investigate the scattering mechanisms and hence to determine the alloy disorder scattering potential in modulation-doped $In_{0.53}Ga_{0.47}As/In_{0.52}Al_{0.48}As$ heterojunction samples with spacer layer thickness in the range from 0 to 400 Å. The experimental data for the temperature dependence of Hall mobility are compared with the electron mobility calculated for major scattering processes by using the theoretical expressions available in the literature. It is found that alloy disorder scattering and polar optical phonon scattering are the dominant scattering mechanisms at low and high temperatures, respectively. However, the effects of acoustic phonon scattering, remote-ionized impurity scattering, background-ionized impurity scattering, and interface roughness scattering on electron mobility are much smaller than that of alloy disorder scattering, at all temperatures. The alloy disorder scattering potential is determined by fitting the experimental data for low-temperature transport mobility of two-dimensional electrons in the first subband of the heterojunction sample with the calculated total mobility.

1. Introduction

The ternary $In_{0.53}Ga_{0.47}As$ alloy lattice-matched to InP substrate has been attracting great interest for use in optoelectronic and microwave devices [1]. The alloy disorder scattering potential (ΔU) is an important parameter that affects the performance of the devices based on $In_{0.53}Ga_{0.47}As$. Previously, several researchers determined the alloy disorder scattering potential for $In_{0.53}Ga_{0.47}As/InP$ and $In_{0.53}Ga_{0.47}As/In_{0.52}Al_{0.48}As$ heterojunctions by comparing the theoretically calculated electron mobility to the experimental data for Hall mobility [2–8]. It has been found that the alloy disorder scattering potential in these heterojunctions takes values in a wide range from 0.4 to 1.1 eV. This approach inevitably introduces undesirable errors, because the measured Hall mobility is not only representative of the lowest sub-band electrons but also includes parallel conduction [9] from electrons in the upper sub-bands and outside the two-dimensional (2D) channel.

The present study is largely motivated by the need for more accurate determination of the alloy disorder scattering potential in $In_{0.53}Ga_{0.47}As/In_{0.52}Al_{0.48}As$ heterojunctions. In this study we used the results of our previous classical magnetotransport [10] and Shubnikov-de Haas (SdH) effect [9] measurements on lattice-matched, modulation-doped $In_{0.53}Ga_{0.47}As/In_{0.52}Al_{0.48}As$ heterojunction samples with undoped spacer layer thickness (t_S) in the range from 0 to 400 Å. The alloy disorder potential is determined by fitting the experimental data for low-temperature transport mobility of 2D electrons in the first subband (rather than the Hall mobility) of each sample to the calculated total mobility that includes the effects of major scattering mechanisms. The present study also provides useful information about the relative importance of various scattering mechanisms that limit the mobility of 2D electrons in these heterojunctions, in the temperature range from 3.3 to 295 K.

*Author to whom all correspondence should be addressed.
†*Present Address*: Department of Physics, Anadolu University, Yunus Emre Campus, 26470 Eskisehir, Turkey.
0022-2461
DOI: 10.1007/s10853-005-1599-2

2. Theoretical background

The calculation of electron mobility in semiconductors is a problem that has been treated by numerical methods such as iterative solution of Boltzmann equation [4] and memory function approximate [11] methods that require the assumption of Matthiessen's rule to obtain the total (combined) scattering-limited mobility. All these calculation techniques are based on the presumption that the scattering mechanisms are mutually independent. Hence many-body effects are ignored, and it is assumed that scattering events are sufficiently infrequent that the electron has no memory of its previous scattering history. The total mobility (μ_{tot}) can be calculated from the scattering-limiting mobilities (μ_j) by using Matthiessen's rule:

$$\frac{1}{\mu_{\text{tot}}} = \sum_j \frac{1}{\mu_j} \tag{1}$$

with

$$\mu_j = \frac{e\tau_j}{m^*} \tag{2}$$

where e is the electronic charge, τ_j is the momentum relaxation time defined for each scattering process and m^* is the electron effective mass. Equation 1 would lead to a more realistic result at low temperatures than at high temperature [2, 12, 13].

The major scattering mechanisms in modulation-doped $In_{0.53}Ga_{0.47}As/In_{0.52}Al_{0.48}As$ heterojunctions are: alloy disorder scattering, acoustic phonon scattering due to the deformation potential coupling, acoustic phonon scattering due to the piezoelectric coupling, polar optical phonon scattering, remote ionized-impurity scattering, background ionized-impurity scattering, interface roughness scattering, and intersubband scattering [7, 14, 15]. In the following, the approximate analytical expressions that we used to calculate the electron mobility limited by each scattering process are briefly outlined for the sake of convenience.

2.1. Alloy disorder scattering

The mobility (μ_A) determined by alloy disorder scattering can be obtained from [14]

$$\mu_A = \frac{16e\,\hbar^3}{m^{*2}\Omega_0\,[\Delta U]^2\,x(1-x)\,3b} \tag{3}$$

where $\hbar$ $(= h/2\pi)$ is the Planck constant, Ω_0 is the average volume of the $In_{0.53}Ga_{0.47}As$ unit cells, ΔU is the alloy disorder scattering potential, x $(= 0.53)$ is the In molar fraction in the $In_{0.53}Ga_{0.47}As$ alloy, and b is the wave function parameter given by [16]

$$b = \left[\left(\frac{12m^*e^2}{\varepsilon\hbar^2}\right)\left(N_{dep} + \frac{11N_{2D}^{(1)}}{32}\right)\right] \tag{4}$$

with

$$N_{dep} = \frac{2\,\varepsilon\,V_b(N_d - N_a)}{e}. \tag{5}$$

Here $N_{2D}^{(1)}$ is the 2D electron density in the first subband of the heterojunction, V_b $(= 0.53$ eV) is the conduction band energy offset, ε is the dielectric permittivity of $In_{0.53}Ga_{0.47}As$, N_d is the donor concentration in the Si-doped $In_{0.52}Al_{0.48}As$ barrier layer, and N_a is the acceptor concentration in the undoped $In_{0.53}Ga_{0.47}As$ layer. The expression in Equation 3 is independent of temperature and dependent upon 2D electron density through the factor b.

2.2. Acoustic phonon scattering

The mobility (μ_{DP}) determined by the scattering of electrons from acoustic phonons generated by the deformation potential can be calculated using [12]

$$\mu_{DP} = \frac{e\hbar^3\rho b' u_l^2}{m^{*2}(E_A)^2 k_B T}\,\frac{1}{I_A(\gamma_l)}. \tag{6}$$

Here ρ is the mass density of $In_{0.53}Ga_{0.47}As$, b' is the effective thickness of the 2D layer in the heterojunction, u_1 is the velocity of longitudinal acoustic phonons, E_A is the acoustic deformation potential, k_B is the Boltzmann constant, T is the absolute temperature, and

$$I_A(\gamma_l) = \left[\left(\frac{4\gamma_l}{3\pi}\right)^2 + 1\right]^{\frac{1}{2}} \tag{7}$$

with

$$\gamma_l = \frac{2\hbar u_l k_F}{k_B T}, \tag{8}$$

where k_F $(= \sqrt{2\pi N_{2D}^{(1)}})$ is the Fermi wavelength of 2D electrons in the first subband.

Lee *et al.* [12] derived the following expression for the ratio of momentum relaxation time (τ_{DP}) for acoustic deformation potential scattering to that (τ_{PE}) for acoustic piezoelectric scattering in a 2D electron gas

$$\frac{\tau_{DP}}{\tau_{PE}} = \frac{b'}{\pi k_F}\left[\frac{9}{32} + \frac{13}{32}\left(\frac{u_l}{u_t}\right)^2 \frac{I_A(\gamma_t)}{I_A(\gamma_l)}\right]\frac{eh_{14}^2}{E_A}. \tag{9}$$

Here h_{14} is the piezoelectric constant, u_t is velocity of transverse acoustic phonons, and

$$I_A(\gamma_t) = \left[\left(\frac{4\gamma_t}{3\pi}\right)^2 + 1\right]^{1/2} \tag{10}$$

with

$$\gamma_t = \frac{2\hbar u_t k_F}{k_B T}. \tag{11}$$

The mobility (μ_{PE}) limited by piezoelectric scattering can be obtained from [12]

$$\mu_{PE} = \mu_{DP}\frac{\tau_{PE}}{\tau_{DP}}. \tag{12}$$

According to Matthiessen's rule, the mobility (μ_{AC}) due to acoustic phonon scattering is given by

$$\mu_{AC} = \left[\frac{1}{\mu_{PE}} + \frac{1}{\mu_{DP}}\right]^{-1}. \tag{13}$$

2.3. Polar optical phonon scattering

Because of the high values of the optical phonon energy, optical phonon scattering in semiconductors is an inelastic process and a momentum relaxation time cannot be defined for polar optical phonon scattering [12, 13]. Nevertheless, the following expression [17] can be used as an approximation to estimate the mobility (μ_{PO}) due to polar optical phonon scattering:

$$\mu_{PO} \cong A \exp\left(\frac{\hbar\omega}{k_B T}\right), \tag{14}$$

where $\hbar\omega$ is the optical phonon energy and A is a proportionality constant that depends on the polar constant, electron effective mass and optical phonon energy [10, 17].

2.4. Remote ionized-impurity scattering

The Coulomb attraction between the 2D electrons in the quantum well and the parent donors in the doped barrier layer of the heterojunction composes a long-range interaction. Therefore, even for lightly doped heterojunction samples, the electrostatic potential contributes to the mobility limitation at low temperatures [14, 15]. Lee *et al.* [12] derived the following expression for the mobility (μ_{RI}) due to remote ionized-impurity scattering

$$\mu_{RI} = \left[\left(\frac{e^3 m^{*2} N_d}{64\pi\hbar^3 \varepsilon^2 k_F^2}\right)\left(\frac{1}{L_0^2} - \frac{1}{L'^2_0}\right)\right]^{-1} \tag{15}$$

with

$$L_0 = Z_1 + t_S \tag{16}$$

$$L'_0 = L_0 + t_d \tag{17}$$

and

$$t_d = \frac{N_{2D}^{(1)}}{N_d}, \tag{18}$$

where Z_1 ($=3/b$) is the average distance of the 2D electron wave function from the heterointerface, t_S is the undoped spacer layer thickness, and t_d is the thickness of the depletion region.

2.5. Background ionized-impurity scattering

The mobility (μ_{BI}) limited by background ionized-impurity scattering can be obtained from [12, 18]

$$\mu_{BI} = \frac{8\pi\hbar^3\varepsilon^2 k_F^2 I_B(\beta)}{e^3 N_{BI} m^{*2}}. \tag{19}$$

Here N_{BI} ($=Z_1 N_d$) is the 2D impurity density in the potential well due to background impurities and/or interface charge,

$$I_B(\beta) = \int_0^{\pi} \frac{\sin^2\theta\, d\theta}{(\sin\theta + \beta)^2} \tag{20}$$

with

$$\beta = \frac{S}{2k_F}, \tag{21}$$

where θ is the scattering angle, and

$$S = \frac{2e^2 m^*}{4\pi\varepsilon\hbar^2} \tag{22}$$

is the screening length [12].

2.6. Interface roughness scattering

Interface roughness (IFR) in layered structures has, in general, been described in terms of a Gaussian distribution of lateral size (Λ) and width (Δ) of the IFR [19–21]. The mobility (μ_{IFR}) of 2D electrons being scattered from IFR can be calculated using [20]

$$\mu_{IFR} = \frac{e}{m^*}\left[\left(\frac{e^2 N_{2D}^{(1)}\Delta\Lambda}{2\varepsilon}\right)^2 \frac{m^*}{\hbar^3} J(k)\right]^{-1} \tag{23}$$

Here

$$J(k) = \int_0^{2k} \frac{\exp(-q^2\Lambda^2/4)}{2k^3(q+q_S)^2\sqrt{1-(q/2k)^2}} q^4 dq, \tag{24}$$

$q = 2k\sin(\theta/2)$, k is the electron wavevector, θ is the scattering angle, and q_S is the screening constant given by

$$q_S = \frac{e^2 m^*}{2\pi\varepsilon\hbar^2} F(q). \tag{25}$$

in which $F(q)$ is the form factor defined by

$$F(q) = \int_0^{\infty} dz \int_0^{\infty} dz' [f(z)]^2 [f(z')]^2 \times \exp(-q|z - z'|) \tag{26}$$

where $f(z)$ is the Fang–Howard variational wave function [22].

3. Experimental data

In this study we used the experimental data for the electronic transport properties of modulation-doped $In_{0.53}Ga_{0.47}As/In_{0.52}Al_{0.48}As$ heterojunction samples obtained from our previous magnetotransport measurements [9, 10]. The heterojunctions were grown by the Molecular Beam Epitaxy (MBE) technique.

GaAs	Undoped	50 Å
$In_{0.52}Al_{0.48}As$	$N_d \sim 10^{24}$ m^{-3} (Si)	250 Å
$In_{0.52}Al_{0.48}As$	Undoped	(t_S=0, 100, 200, and 400 Å)
$In_{0.53}Ga_{0.47}As$	Undoped	6000 Å
$In_{0.53}Ga_{0.47}As$	$N_a \sim 10^{23}$ m^{-3} (Be)	2000 Å
InP (Fe) substrate	Semi-insulating	

Figure 1 The structure of the modulation-doped $In_{0.53}Ga_{0.47}As$ /$In_{0.52}Al_{0.48}As$ heterojunctions samples used in the study.

Layer structure and doping parameters of all the samples were nominally identical except for the undoped $In_{0.52}Al_{0.48}As$ spacer layer thickness which was varied from 0 (no spacer layer) to 400 Å (Fig. 1). In these structures the 2D-electron gas is confined within the undoped $In_{0.53}Ga_{0.47}As$ layer near the heterojunction interface.

The classical magnetotransport (electrical resistance, low-field Hall effect and magnetoresistance) measurements were made for each sample as a function of temperature from 3.3 to 295 K in a three-stage closed-cycle refrigeration system using a conventional dc technique [10]. SdH effect measurements were carried out in the temperature range between 3.3 and 20 K at applied magnetic fields up to 2.3 T [9]. In all the measurements, which were made in the dark, the dc current flowing through the sample was low enough to ensure ohmic conditions. The current flow was in the plane of the 2D-electron gas and the magnetic field was applied perpendicular to it. The results of classical magnetotransport measurements were used to determine the Hall mobility and Hall carrier density of the samples. The SdH effect measurements on the samples with spacer layer thickness t_S = 0, 100 and 200 Å showed that the first and the second subbands were already populated with 2D electrons even at 3.3 K [9]. However, for the samples with t_S = 400 Å, only the first subband was populated. The parallel conduction in the later samples was shown [9] to be due to bulk charge carriers outside the 2D-channel (i.e., 3D electrons in undepleted donors in the barrier layer). The Hall mobility, Hall carrier density, and the carrier density, effective mass and transport mobility of 2D electrons in the first and the second subbands of the samples studied are given in Table I.

The transport mobility of 2D electrons in each subband was determined [9] from the magnetoresistance measurements in the classical regime. All the samples exhibited positive magnetoresistance at low magnetic fields, well below the onset of SdH oscillations. The positive magnetoresistance evinces for the presence of parallel conducting channels in the heterojunction samples [23, 24]. The low-field magnetoresistance data were fitted to a two-band model [23–25] with the measured values of carrier density and effective mass of 2D electrons in each subband as input parameters and by taking the transport mobilities μ_{t1} and μ_{t2} as adjustable parameters. The transport mobilities μ_{t1} and μ_{t2} of 2D electrons in the first and second subbands in the samples with $t_S = 0$, 100 and 200 Å were determined [9] with an accuracy of better than 1%. For the sample with $t_S = 400$ Å, Tiraş *et al*. [9] obtained $\mu_{t1} = 9.16$ m^2/V.s for 2D electrons in the first subband and $\mu_{3D} = 0.052$ m^2/V.s for charge carriers in the parallel conducting channel. The very small value ($= 0.052$ m^2/V.s) found for μ_{3D} was comparable to the mobility measured [26, 27] for 3D electrons (with an effective mass of $0.089m_0$) in Si-doped $In_{0.52}Al_{0.48}As$ epitaxial layers with a doping level similar to our samples. Therefore, Tiraş *et al*. [9] concluded that the parallel conduction giving rise to the strong positive magnetoresistance for the sample with $t_S = 400$ Å was due to undepleted donors in Si-doped $In_{0.52}Al_{0.48}As$ barrier. For further details of data analysis refer to [9] and [10].

4. Results and discussion

In the calculation of the scattering-limited electron mobility we used the values for the effective mass and carrier density of 2D electrons in the first subband of the modulation-doped $In_{0.53}Ga_{0.47}As/In_{0.52}Al_{0.48}As$ heterojunction samples (Table I). The other physical parameters of bulk $In_{0.53}Ga_{0.47}As$ (Table II) are taken from the literature [1, 7, 28–29]. We have no experimental evidence for the lateral size (Λ) and the width (Δ) of the interface roughness (IFR) in our samples. Therefore, in order to calculate the mobility determined by IFR scattering, we used Δ = 2.8 Å and Λ = 100 Å for IFR at the $In_{0.53}Ga_{0.47}As/In_{0.52}Al_{0.48}As$ interface, which were deduced from photoluminescence measurements on $In_{0.53}Ga_{0.47}As/In_{0.52}Al_{0.48}As$ single quantum well samples of similar optical quality to ours [30]. The results we obtained for the scattering-limited

TABLE I The Hall mobility, Hall carrier density, total 2D carrier density, and the carrier density, effective mass and transport mobility of 2D electrons in the first and second subbands of the modulation-doped $In_{0.53}Ga_{0.47}As/In_{0.52}Al_{0.48}As$ heterojunction samples measured at 3.3 K (data taken from [9, 10])

Sample	MV572A	MV576A	MV577	MV578A
Spacer thickness, t_S (Å)	0	100	200	400
Hall mobility, μ_H (m^2 V^{-1} s^{-1})	4.8	8.1	6.7	4.1
Hall carrier density, N_H (10^{16} m^{-2})	1.95	1.10	0.91	1.13
Total 2D carrier density, N_{2D} (10^{16} m^{-2})	2.00	1.30	0.98	0.51
2D carrier density in the 1st subband, $N_{2D}^{(1)}$ (10^{16} m^{-2})	1.67	1.09	0.86	0.51
2D carrier density in the 2nd subband, $N_{2D}^{(2)}$ (10^{16} m^{-2})	0.33	0.21	0.12	–
Effective mass of 2D electrons in the 1st subband, m^* (m_0)	0.041	0.041	0.039	0.042
Transport mobility of 2D electrons in the 1st subband, μ_{t1} (m^2 V^{-1} s^{-1})	4.91	7.54	6.92	9.16
Transport mobility of 2D electrons in the 2nd subband, μ_{t2} (m^2 V^{-1} s^{-1})	3.75	3.30	1.08	–

TABLE II $In_{0.53}Ga_{0.47}As$ material parameters used in the calculation of electron mobility [1, 7, 28, 29]

Lattice constant, a (Å)	5.8687
Mass density, ρ (kg m^{-3})	5490
Static dielectric constant, ε (ε_0)	13.5
Velocity of transverse acoustic phonons, u_t (m s^{-1})	4260
Velocity of longitudinal acoustic phonons, u_l (m s^{-1})	4810
Acoustic deformation potential, E_A (eV)	9.4
Piezoelectric constant, h_{14} (V m^{-1})	2.77×10^8

electron mobilities (Table III) demonstrate that, at low temperatures, the mobilities determined by all scattering mechanisms, except the alloy disorder scattering, are at least an order of magnitude higher than the measured Hall mobility. According to Matthiessen's rule, the contribution of higher mobility to the total mobility (μ_{tot}) is less than that of lower mobility. Therefore, at low temperatures, both the Hall mobility and the transport mobility of 2D electrons in the modulation-doped $In_{0.53}Ga_{0.47}As/In_{0.52}Al_{0.48}As$ heterojunctions are determined primarily by alloy disorder scattering. Intersubband scattering [16, 31] should also be considered in the case of heterojunction samples with double-subband occupancy (i.e., with t_S = 0, 100, and 200 Å). However, previous calculations [15] of the electron mobility in modulation-doped $In_{0.53}Ga_{0.47}As/In_{0.52}Al_{0.48}As$ heterojunctions with $t_S = 80$ Å showed that the effects of intersubband scattering on the electron mobility are not as prominent as those of alloy disorder scattering.

We determined the alloy disorder scattering potential (ΔU) by fitting the calculated total mobility (Equation 1) to the transport mobility of 2D electrons in the first subband of each sample measured at 3.3 K. In this procedure ΔU was taken as an adjustable parameter. The values thus obtained for ΔU in the modulation-doped $In_{0.53}Ga_{0.47}As/In_{0.52}Al_{0.48}As$ heterojunctions are essentially independent of the spacer layer thickness (Table III), although the density of 2D electrons in the first subband decreased systematically as the spacer layer thickness was increased from 0 to 400 Å (see Table I). The mobility (μ_A) determined by alloy disorder scattering, as calculated by using the best-fit values of ΔU in Equation 3, and the total mobility (μ_{tot}) are also included in Table III.

The values we obtained for the alloy disorder scattering potential in modulation-doped $In_{0.53}Ga_{0.47}As/In_{0.52}Al_{0.48}As$ heterojunctions with spacer layer thickness $t_S = 0$, 100, 200 and 400 Å are comparable to those reported in the literature for various $In_{0.53}Ga_{0.47}As/InP$ and $In_{0.53}Ga_{0.47}As/ In_{0.52}Al_{0.48}As$ heterostructures [3–7]. Basu *et al.* [4] calculated the electron mobility in $In_{0.53}Ga_{0.47}As/InP$ using Boltzmann equation that was solved by a numerical iterative technique and determined the alloy disorder scattering potential by fitting the calculated mobility to the experimental Hall mobility. They found that the alloy scattering potential falls in a range from 0.7 to 1.0 eV for different samples. Matsuoka *et al.* [7] determined the alloy disorder scattering potential as 0.65 eV and 0.85 eV by fitting the calculated mobility to the experimental Hall mobility for two different $In_{0.53}Ga_{0.47}As/In_{0.52}Al_{0.48}As$ single heterostructures with doping densities in the barrier layer of 3×10^{23} m^{-3} and 1×10^{24} m^{-3}, but both with $t_S = 0$ Å. Kobayashi *et al.* [6] carried out Monte Carlo simulation to investigate the electron transport in $In_{0.53}Ga_{0.47}As/In_{0.52}Al_{0.48}As$ single heterostructures by taking into account the effects of major scattering mechanisms. By comparing the calculated mobility with low-field Hall mobility data they found that the alloy disorder scattering potential is about 0.78 eV.

Recently, Vasileska *et al.* [8] investigated the gate voltage dependence of the low-field electron mobility in a modulation-doped $In_{0.53}Ga_{0.47}As/In_{0.52}Al_{0.48}As$ heterostructure with double-subband occupancy (t_S = 100 Å) by using a real-time Green's function formalism. They found that the electron mobility decreased from 29 to 14 m^{2}V^{-1}s^{-1} when the alloy disorder scattering potential increased from 0.4 eV to 0.6 eV (Fig. 2). The values obtained in this study for the alloy disorder scattering potential of modulation-doped $In_{0.53}Ga_{0.47}As/In_{0.52}Al_{0.48}As$ heterojunction samples with double-subband occupancy (i.e., with t_S = 0, 100, and 200 Å) are in reasonable agreement with the results of real-time Green's function formalism [8] as extrapolated to mobilities below 10 m^{2}V^{-1}s^{-1} (Fig. 2).

The figures within brackets in the last raw of Table III correspond to the alloy disorder scattering potential (ΔU) estimated by fitting the calculated total mobility to the Hall mobility measured at 3.3 K. For each of the samples with double-subband occupancy, the values obtained for ΔU by using either the transport mobility of 2D electrons in the first subband (μ_{t1}) or the Hall mobility (μ_H) are very close to each other. However, for the sample with t_S = 400 Å, the two values of ΔU differ by about 45%. This is because of the large difference between the values found for μ_{t1} and μ_H (see Table I). In this particular sample, the parallel conduction due to low-mobility 3D electrons

TABLE III Scattering-limited mobilities and alloy disorder scattering potential for modulation-doped $In_{0.53}Ga_{0.47}As/In_{0.52}Al_{0.48}As$ heterojunction samples determined at $T = 3.3$ K

Spacer thickness, t_S (Å)	0	100	200	400
Z_1 (Å)	68.6	77.7	85.6	99.5
Transport mobility of 2D electrons in the 1st subband, μ_{t1} (m^2 V^{-1} s^{-1})	4.91	7.54	6.92	9.16
Calculated total mobility, μ_{tot} (m^2 V^{-1} s^{-1})	4.8	7.7	7.0	9.3
Alloy disorder scattering mobility, μ_A (m^2 V^{-1} s^{-1})	5.5	8.3	7.4	10.7
Acoustic phonon scattering mobility, μ_{AC} (m^2 V^{-1} s^{-1})	600	720	950	1100
Remote ionized-impurity scattering mobility, μ_{RI} (m^2 V^{-1} s^{-1})	46	190	560	1500
Background ionized-impurity scattering mobility, μ_{BI} (m^2 V^{-1} s^{-1})	610	280	210	79
Interface roughness scattering mobility, μ_{IFR} (m^2 V^{-1} s^{-1})	89	103	110	129
Alloy disorder scattering potential, ΔU (eV)	1.01 (0.99)	0.81 (0.78)	0.91 (0.92)	0.81 (1.17)

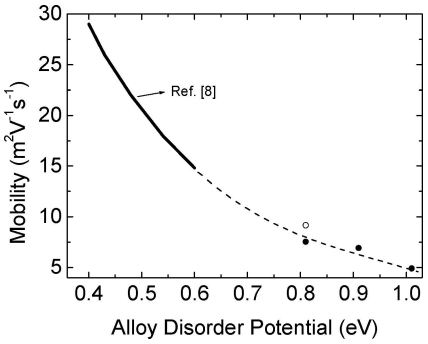

Figure 2 Variation of electron mobility with alloy disorder scattering potential in modulation-doped $In_{0.53}Ga_{0.47}As/In_{0.52}Al_{0.48}As$ heterojunctions. The solid line represents the results of real-time Green's function formalism [8] and the dashed line is an extrapolation of these results. The full and open circles correspond to the transport mobility of 2D electrons in the first subband of the heterojunction samples with double-subband (t_S = 0, 100, 200 Å) and single-subband (t_S = 400 Å) occupancy, respectively.

in undepleted donors in the barrier layer lowered significantly the Hall mobility [9]. The results suggest that for the modulation-doped $In_{0.53}Ga_{0.47}As/In_{0.52}Al_{0.48}As$ heterojunction samples, in which the measured Hall mobility includes the effects of parallel conduction from charge carriers outside the 2D channel, the use of Hall mobility in the determination of the alloy disorder scattering potential overestimates markedly the value of ΔU.

The calculated scattering-limited mobilities μ_A, μ_{RI}, μ_{BI}, μ_{IFR}, μ_{AC}, μ_{PO} and μ_{tot} are compared in Fig. 3 with the Hall mobility measured for the modulation-doped $In_{0.53}Ga_{0.47}As/\ In_{0.52}Al_{0.48}As$ heterojunction samples, in the temperature range from 3.3 to 295 K. The Hall mobility of each sample is essentially independent of temperature below about 70 K. This finding indicates that the transport mobility of 2D electrons is determined by temperature insensitive scattering mechanisms such as alloy disorder scattering and interface roughness scattering. However, as Fig. 3 illustrates the electron mobility is limited primarily by alloy disorder scattering at low temperatures ($T < 90$ K) and by polar optical phonon scattering and alloy disorder scattering at higher temperatures. The effects of acoustic phonon scattering, remote ionized-impurity scattering, background ionized-impurity scattering and interface roughness scattering on the electron mobility are estimated to be much smaller at all temperatures than those of alloy disorder scattering.

5. Conclusions

Experimentally determined electron transport mobility is compared with those calculated using all the major scattering mechanisms in modulation-doped $In_{0.53}Ga_{0.47}As/In_{0.52}Al_{0.48}As$ heterojunction samples with spacer layer thickness in the range from 0 to 400 Å. In the calculations we used approximate analytical expressions available in the literature. The results suggest strongly that the combined effects of acoustic phonon scattering, remote ionized-impurity scattering, background-ionized impurity scattering and interface roughness scattering on the transport mobility of 2D electrons are orders of magnitude smaller than those of alloy disorder scattering and hence the electron mobility is limited primarily by alloy disorder scattering at low temperatures ($T < 90$ K). It is determined, however, by polar optical phonon scattering and alloy disorder scattering at higher temperatures. The alloy disorder scattering potential is determined by fitting the cal-

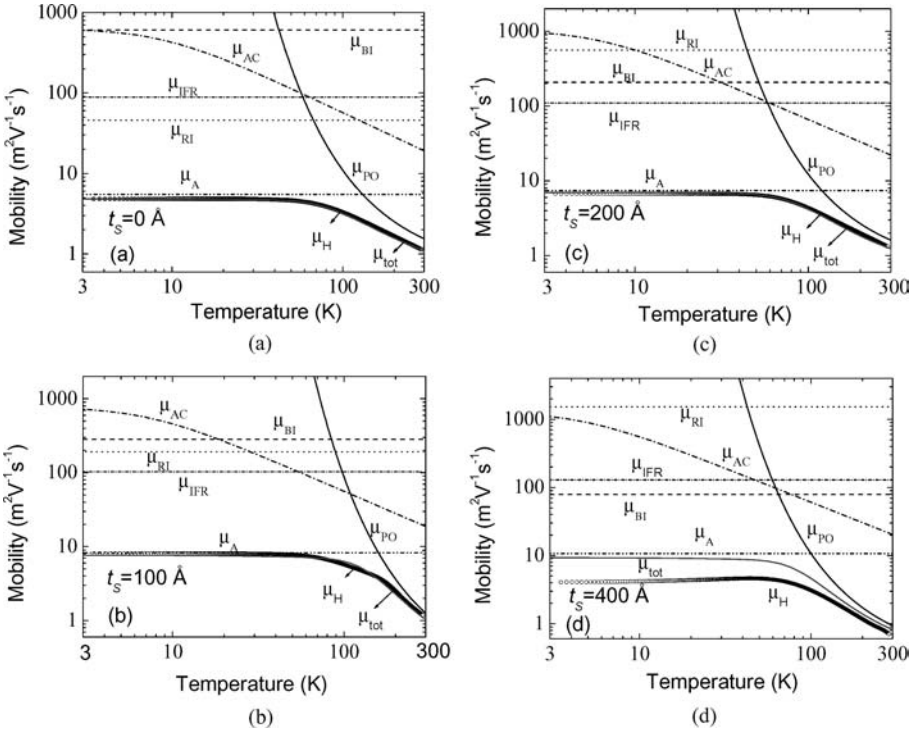

Figure 3 Temperature dependence of the Hall mobility (μ_H) measured [10] at a magnetic field of 1.0 T and alloy disorder scattering mobility (μ_A), acoustic phonon scattering mobility (μ_{AC}), remote ionized-impurity scattering mobility (μ_{RI}), background ionized-impurity scattering mobility (μ_{BI}), interface roughness scattering mobility (μ_{IFR}), polar optical phonon scattering mobility (μ_{PO}), total mobility (μ_{tot}) for the modulation-doped $In_{0.53}Ga_{0.47}As/In_{0.52}Al_{0.48}As$ heterojunctions with spacer layer thickness (a) t_S = 0 Å, (b) t_S = 100 Å, (c) t_S = 200 Å, and (d) t_S = 400 Å.

culated total mobility to the low-temperature transport mobility of 2D electrons in the first subband. It is found that the alloy disorder scattering potential takes values in the range 0.81–1.01 and is essentially independent of the spacer layer thickness. The results show clearly that for the heterojunction samples, in which the measured Hall mobility includes the effects of parallel conduction due to electrons outside the 2D channel, the use of Hall mobility overestimates significantly the alloy disorder scattering potential.

References

1. P. BHATTACHARYA, "Properties of Lattice-Matched and Strained Indium Gallium Arsenide" (INSPEC, London, 1993).
2. Y. TEKADA and T. P. PEARSALL, *Electron. Lett.* **17** (1981) 574.
3. G. BASTARD, *Appl. Phys. Lett.* **43** (1983) 591.
4. P. K. BASU and B. R. NAG, *ibid.* **43** (1983) 689.
5. P. K. BASU, D. CHATTOPADHYAY and C. K. SARKAR, *J. Phys. C: Solid State Phys.* **19** (1986) L173.
6. E. KOBAYASHI, T. MATSUOKA, K. TANIGUCHI and C. HAMAGUCHI, *Solid-State Electron.* **32** (1989) 1845.
7. T. MATSUOKA, E. KOBAYASHI, K. TANIGUCHI, C. HAMAGUCHI and S. SASA, *Jpn. J. Appl. Phys.* **29** (1990) 2017.
8. D. VASILESKA, C. PRASAD, H. H. WIEDER and D. K. FERRY, *Phys. Stat. Sol B* **239** (2003) 103.
9. E. TIRAŞ, M. CANKURTARAN, H. ÇELİK, A. BOLAND THOMS and N. BALKAN, *Superlattices Microstruct.* **29** (2001) 147.
10. S. ALTINÖZ, E. TIRAS, A. BAYRAKLI, H. CELIK, M. CANKURTARAN and N. BALKAN, *Phys. Status Solidi A* **182** (2000) 717.
11. J. E. HASBUN, *Phys. Rev. B* **52** (1995) 11989.
12. K. LEE, M. SHUR, T. J. DRUMMOND and H. MORKOC, *J. Appl. Phys.* **54** (1983) 6432.
13. J. J. HARRIS, J. A. PALS and R. WOLTER, *Rep. Prog. Phys.* **52** (1989) 1217.
14. G. BASTARD, "Wave Mechanics Applied to Semiconductor Heterostructures, Les Editions de Physique" (Les Ulis, 1988).
15. W. WALUKIEWICZ, H. E. RUDA, J. LAGOWSKI and H. C. GATOS, *Phys. Rev. B* **30** (1984) 4571.
16. T. ANDO, A. B. FOWLER and F. STERN, *Rev. Mod. Phys.* **54** (1982) 437.
17. K. SEEGER, "Semiconductor Physics —An Introduction, 6th ed." (Springer-Verlag, New York, 1997).
18. K. HESS, *Appl. Phys. Lett.* **35** (1979) 484.
19. H. SAKAKI, T. NODA, K. HIRIKAWA, M. TANAKA, and T. MATSUSUE, *ibid.* **51** (1987) 1934.
20. N. BALKAN, R. GUPTA, M. E. DANIELS, B. K. RIDLEY, and M. EMENY, *Semicond. Sci. Technol.* **5** (1990) 986.
21. B. K. RIDLEY, B. E. FOUTZ, and L. F. EASTMAN, *Phys. Rev. B* **61**, (2000) 16862.
22. K. HIRAKAWA, H. SAKAKI and J. YOSHINO, *Appl. Phys. Lett.* **45** (1984) 253.
23. M. J. KANE, N. APSLEY, D. A. ANDERSON, L. L. TAYLOR and T. KERR, *J. Phys. C: Solid State Phys.* **18** (1985) 5629.
24. J. J. HARRIS, J. M. LAGEMAA, S. J. BATTERSBY, C. M. HELLON, C. T. FOXON and D. E. LACKLISON, *Semicond. Sci. Technol.* **3** (1988) 773.
25. S. J. BATTERSBY, F. M. SELTEN, J. J. HARRIS and C. T. FOXON, *Solid-State Electron.* **31** (1988) 1083.
26. K. Y. CHENG, A. Y. CHO and W. R. WAGNER, *J. Appl. Phys.* **52** (1981) 6328.
27. T. TANAHASHI, K. NAKAJIMA, A. YAMAGUCHI, and I. UMEBU, *Appl. Phys. Lett.* **43** (1983) 1030.
28. A. J. STRAW VICKERS and J. S. ROBERTS, *Solid-State Electron.* **32** (1989) 1539.
29. T. P. PEARSALL, "GaInAsP Alloy Semiconductors "1st ed." (Wiley, New York, 1982).
30. F. Y. JUANG, P. K. BHATTACHARYA and J. SINGH, *Appl. Phys. Lett.* **48** (1980) 290.
31. S. MORI and T. ANDO, *J. Phys. Soc. Jpn.* **48** (1980) 865.

Received 17 February
and accepted 15 April 2005